Accurate Impedance Based Fault Location Algorithm Using Communication between Protective Relays

Cezary Dzienis,
Yilmaz Yelgin
EM EA PRO D
Siemens AG
Berlin, Germany
cezary.dzienis@siemens.com

Marie Washer
Jean-Claude Maun
École Polytechnique de Bruxelles
Université Libre de Bruxelles
Brussels, Belgium
marie.washer@ulb.ac.be

***Abstract*— The reactance method with fault resistance separation has been developed in order to determine as precisely as possible the impedance of a fault loop in a transmission or distribution power system line. This method has commonly been used for impedance calculation in case of a single phase-to-earth fault in diverse power system protection applications. New developments in this area have shown that the extension of the method to multi-phase faults is not only possible but also of practical relevance. This research consists in an improvement of this calculation method using data from both the own and the remote line end. This approach uses communication between two measurement units e.g. protection relays, which have the advantage of not requiring a precise synchronization with each other. The additional time invariant parameters of the power system, acquired by each device and transferred to the remote end, allow an exact computation of the fault reactance and fault resistance. In this paper, the derivation of this novel approach as well as experimental results in a fault location application are presented.**

Keywords*— *Fault Location, Impedance Measurement, Power System Protection, Transmission / Distribution Line

I. INTRODUCTION

Fault location algorithms give an estimation of the distance between the point of measurement at the device (mostly protective relay) and the point of a short circuit (fault) in a transmission or distribution line. The maintenance effort of the line after an already cleared temporary fault and the recovery time of the line after a permanent fault both depend on the accuracy of the fault location. As a result, the fault location function contributes indirectly to an improvement in quality and availability of electrical energy. Accuracy of the fault location depends on the chosen algorithm and hypothesis for the calculation itself, as well as on the complexity of the power system and on fault conditions.

This paper focuses on the double-ended impedance based fault location algorithm, which is derived from the reactance method with fault resistance separation. The fault location method described in this paper is based on the computation of the faulty loop's reactance, which is linearly proportional to the distance to the fault.

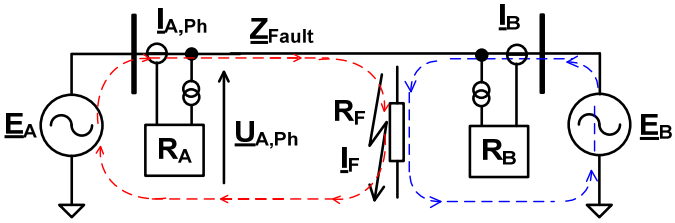

Figure 1. Fault with transition resistance in a double side supplied line

A faulty doubly in-fed line is first considered in the form of a single-phase system (Fig. 1). For the short circuit, a purely resistive fault is adopted. If the faulty loop includes a fault resistance R_F, it is not possible to calculate the exact reactance value using only the measurements from one side A or B. Indeed, the unknown fault current $\underline{I}_F$ is necessary for the calculation. Applying Kirchhoff's Voltage Law (KVL) to the system from the point of view of side A results in (1), which is the base to extract the fault reactance and resistance:

$$\underline{U}_{A,Ph} = \underline{Z}_{Fault} \cdot \underline{I}_{A,Ph} + R_F \cdot \underline{I}_F \qquad (1)$$

In order to eliminate from (1) the unknown voltage drop on the transition resistance, which depends on the fault current, the so called load decoupled compensation quantity $\underline{I}_{A,Cmp}$ and compensation factor $\underline{\delta}_{A,B}$ are introduced. $\underline{I}_{A,Cmp}$ corresponds to the fault current as it is seen from side A, and $\underline{\delta}_{A,B}$ is an extension factor for the double in-fed line. The factor $\underline{\delta}_{A,B}$ corresponds to the phase shift due to the consideration of the remote end and is therefore the most influent term of the compensation. The product of these two quantities gives an estimation of the fault current $\underline{I}_F$. Therefore, it is considered that this term has the same electric phase angle and magnitude as the fault current $\underline{I}_F$. Equation (1) is multiplied by the conjugate of these combined quantities. The term reflecting the resistive voltage drop in (1) becomes a pure real number and can be eliminated by considering only the imaginary part.

$$\mathrm{Im}[\underline{U}_{A,Ph} \cdot \underline{I}^{*}_{A,Cmp} \cdot \underline{\delta}^{*}_{A,B}] = \mathrm{Im}[\underline{Z}_{Fault} \cdot \underline{I}_{A,Ph} \cdot \underline{I}^{*}_{A,Cmp} \cdot \underline{\delta}^{*}_{A,B}] \quad (2)$$

Introducing the line's angle φ and thereby isolating the reactance X_{Fault} from the fault impedance $\underline{Z}_{fault}$, equation (3) is obtained. This result is proportional to the fault location.

$$X_{Fault} = \frac{\sin\varphi \cdot \mathrm{Im}[\underline{U}_{A,Ph} \cdot \underline{I}^{*}_{A,Cmp} \cdot \underline{\delta}^{*}_{A,B}]}{\mathrm{Im}[e^{j\varphi} \cdot \underline{I}_{A,Ph} \cdot \underline{I}^{*}_{A,Cmp} \cdot \underline{\delta}^{*}_{A,B}]} \quad (3)$$

The compensation quantity and extension factor can further be used to determine the fault's resistance R_F. Replacing the fault current by the product of these two quantities in (1), and multiplying by the conjugated product of the fault impedance and phase current $\underline{Z}_{Fault}{}^{*}\,\underline{I}_{A,Ph}{}^{*}$, the voltage drop on the fault impedance can be eliminated and the fault resistance can be extracted:

$$R_F = \frac{\mathrm{Im}[\underline{U}_{A,Ph} \cdot e^{-j\varphi} \cdot \underline{I}^{*}_{A,Ph}]}{\mathrm{Im}[\underline{I}_{A,Cmp} \cdot \underline{\delta}_{A,B} \cdot e^{-j\varphi} \cdot \underline{I}^{*}_{A,Ph}]} \quad (4)$$

II. Impedance Measurement in Power Systems

Each fault type in the symmetrical electrical power system can be described with symmetrical components. The zero-, negative- and delta-positive- sequence components are independent from the load flow. This property is used to introduce compensation quantities and thereby to eliminate the voltage drop on the fault resistance in order to achieve a precise reactance value. The previously introduced extension factor is calculated based on the symmetrical components equivalent circuit as well.

The phase voltage $\underline{U}_{A,Ph}$ and phase current $\underline{I}_{A,Ph}$ respectively represent the voltage and current in the considered single-phase fault loop. In the case of a phase-to-earth fault, the earth compensation factor $\underline{k}_0$ is introduced, similarly to the conventional fault location algorithm, to take into account the earth return path, as shown in (5)-(6).

$$X_{Fault} = \frac{\sin\varphi \cdot \mathrm{Im}[\underline{U}_{A,Ph-E} \cdot \underline{I}^{*}_{A,Cmp} \cdot \underline{\delta}^{*}_{A,B}]}{\mathrm{Im}[e^{j\varphi} \cdot (\underline{I}_{A,Ph} - \underline{k}_0 \underline{I}_{A,E}) \cdot \underline{I}^{*}_{A,Cmp} \cdot \underline{\delta}^{*}_{A,B}]} \quad (5)$$

$$R_F = \frac{\mathrm{Im}[\underline{U}_{A,Ph} \cdot e^{-j\varphi} \cdot (\underline{I}_{A,Ph} - \underline{k}_0 \underline{I}_{A,E})^{*}]}{\mathrm{Im}[\underline{I}_{A,Cmp} \cdot \underline{\delta}_{A,B} \cdot e^{-j\varphi} \cdot \underline{I}^{*}_{A,Ph}]} \quad (6)$$

In Fig. 2, the single phase to earth fault in symmetrical components is represented. It can be concluded that the fault current $\underline{I}_F$ can be reflected by positive, negative or zero sequence current. Since the negative and zero sequence currents are independent from the load flow, both these components can be used as compensation quantities. In order to estimate the fault current $\underline{I}_F$ using the sequence current measured on one network side, appropriate compensation factors must be introduced.

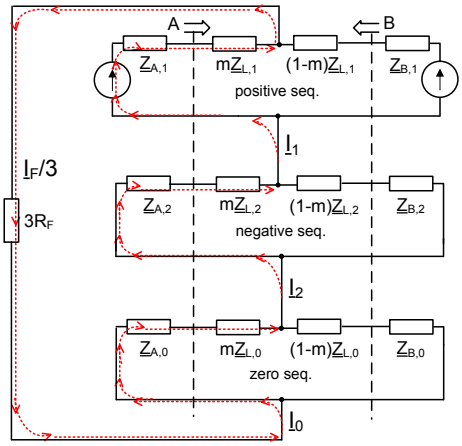

Figure 2. Single phase-to-earth fault with fault resistance (representation in symmetrical components – double side supplied line)

This compensation factor can be derived from the system impedances. Applying the KVL for the zero sequence circuit, the following expression can be obtained:

$$\left[\underline{Z}_{A,0} + m \cdot \underline{Z}_{L,0}\right] \cdot \underline{I}_{A,0} = \left[(1-m) \cdot \underline{Z}_{L,0} + \underline{Z}_{B,0}\right] \cdot \underline{I}_{B,0} \quad (7)$$

From the sequence equivalent circuit one can conclude:

$$\underline{I}_F = 3 \cdot (\underline{I}_{A,0} + \underline{I}_{B,0}) \quad (8)$$

Describing the unknown current $\underline{I}_{B,0}$ of the opposite side with the measured current $\underline{I}_{A,0}$ of the own side (7) and substituting it into (8), the following expression can be written:

$$\underline{I}_F = 3I_{A,0} \cdot \left(\frac{\underline{Z}_{A,0} + m \cdot \underline{Z}_{L,0}}{(1-m) \cdot \underline{Z}_{L,0} + \underline{Z}_{B,0}} + 1 \right) \quad (9)$$

$$\underline{I}_F = \underline{I}_{A,Cmp}\, \underline{\delta}_{A,B}$$

As a result, the compensation factor $\underline{\delta}_{A,B}$ and compensation current $\underline{I}_{A,Cmp}=3\underline{I}_{A,0}$ can be identified. An analogue consideration can be carried out for the negative and delta-positive components.

For phase-to-phase faults, the voltage and current to take into account consist in the voltage (respectively current) difference between the two concerned phases. This method can be generalized for phase-to-phase faults with earth [6], [7]. The corresponding reactance and resistance are given in (10) and (11).

$$X_{Fault} = \frac{\sin\varphi \cdot \mathrm{Im}[\underline{U}_{A,Ph1-Ph2} \cdot \underline{I}^{*}_{A,Cmp} \cdot \underline{\delta}^{*}_{A,B}]}{\mathrm{Im}[e^{j\varphi} \cdot \underline{I}_{A,Ph1-Ph2} \cdot \underline{I}^{*}_{A,Cmp} \cdot \underline{\delta}^{*}_{A,B}]} \quad (10)$$

$$R_F = \frac{\mathrm{Im}[\underline{U}_{A,Ph1-Ph2} \cdot e^{-j\varphi} \cdot \underline{I}^{*}_{A,Ph1-Ph2}]}{\mathrm{Im}[\underline{I}_{A,Cmp} \cdot \underline{\delta}_{A,B} \cdot e^{-j\varphi} \cdot \underline{I}^{*}_{A,Ph1-Ph2}]} \quad (11)$$

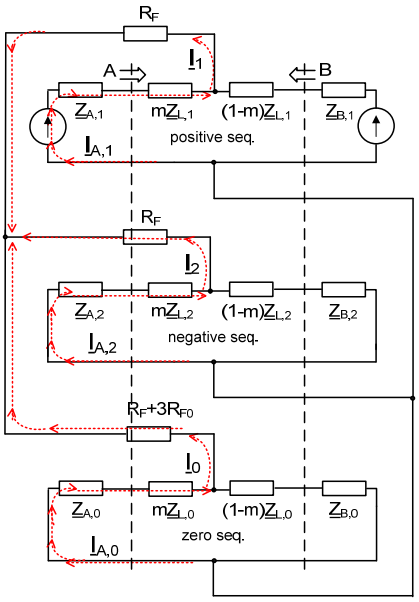

Figure 3. Phase-phase-to-earth fault with fault resistance (representation in symmetrical components)

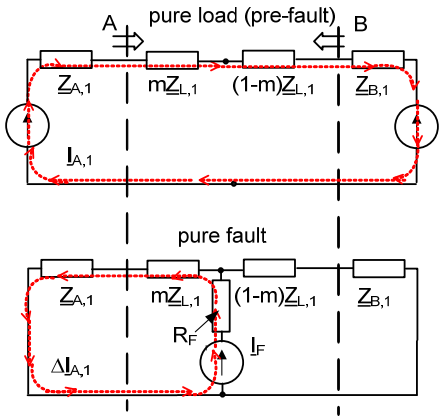

Figure 4. Three phase fault with symmetrical fault resistance (superposition principle)

Fig. 3 presents the phase-to-phase fault with earth in symmetrical components. It is assumed that the fault resistance between phases $2R_F$ is split symmetrical by the earth fault resistance R_{F0}. Expressing the fault current as the difference between both phase currents flowing into the fault, the following generalization can be made:

$$\underline{I}_{F,Ph1} - \underline{I}_{F,Ph2} = \underline{I}_F = \left[\underline{I}_{A,Cmp,2} \quad -\underline{I}_{A,Cmp,0}\right] \cdot \begin{bmatrix} \underline{\delta}_{A,B,2} \\ \underline{\delta}_{A,B,0} \end{bmatrix} \quad (12)$$

Since in case of a phase-to-phase fault, the zero sequence current is zero, the formulation from (12) is still valid.
For three phase faults, the positive sequence current and voltage are used:

$$X_{Fault} = \frac{\sin\varphi \cdot \mathrm{Im}[\underline{U}_{A,1} \cdot \underline{I}^*_{A,Cmp} \cdot \underline{\delta}^*_{A,B}]}{\mathrm{Im}[e^{j\varphi} \cdot \underline{I}_{A,1} \cdot \underline{I}^*_{A,Cmp} \cdot \underline{\delta}^*_{A,B}]} \quad (13)$$

$$R_F = \frac{\mathrm{Im}[\underline{U}_{A,1} \cdot e^{-j\varphi} \cdot \underline{I}^*_{A,1}]}{\mathrm{Im}[\underline{I}_{A,Cmp} \cdot \underline{\delta}_{A,B} \cdot e^{-j\varphi} \cdot \underline{I}^*_{A,1}]} \quad (14)$$

For the calculation of the compensation factor, the approach with superimposed components must be used (Fig. 4). The compensation quantity is the difference between the current in pre-fault and fault condition, in positive sequence. This current will further be called delta current. It is also assumed that the fault is symmetrical, with a resistance R_F between each phase and the star point.
Depending on the type of fault and implicated phases, the quantity and compensation factor can be determined using the adapted symmetrical components.

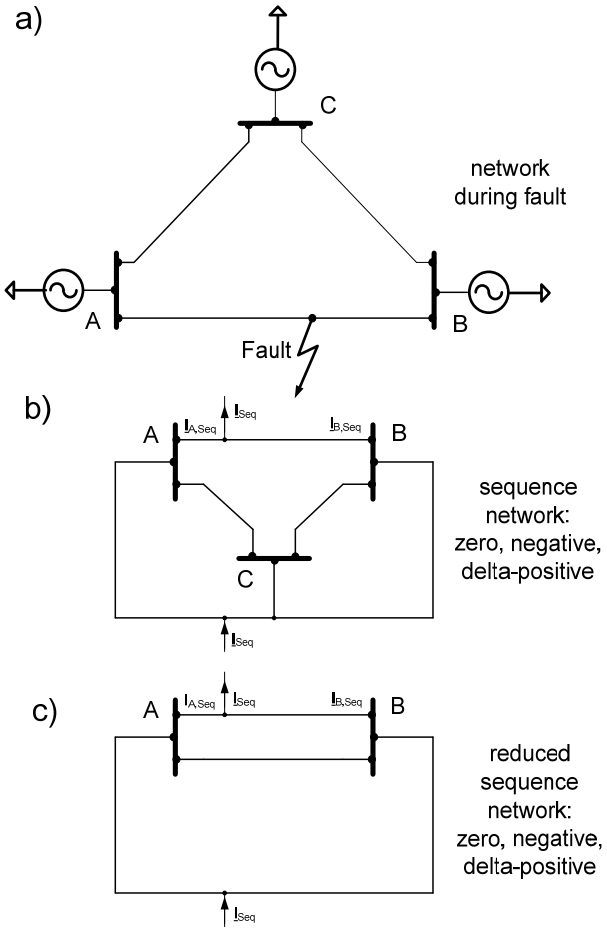

Figure 5. Meshed power system with fault on the line between busbars A and B a) network during fault; b) sequence network; c) reduced sequence network

The line data used in the computation of the compensation factors is available in the relay device. However, the source impedances are not parameterized in common protection devices. These network parameters can be computed using the measurements made by the protection relays during the fault

transient. Considering the equivalent circuits in symmetrical components, it can be concluded that based on the measured voltages and currents, in case of the fault on the line, the real source impedance can be simply calculated:

$$\underline{Z}_{A,0} = -\frac{\underline{U}_{A,0}}{\underline{I}_{A,0}}, \underline{Z}_{A,2} = -\frac{\underline{U}_{A,2}}{\underline{I}_{A,2}}, \quad \underline{Z}_{A,1} = -\frac{\Delta\underline{U}_{A,1}}{\Delta\underline{I}_{A,1}} \tag{15}$$

This method can also be used in meshed networks however in that case, the calculated impedances do not reflect the real source impedances. As a proof, the power system from Fig. 5a can be used. Each meshed system can be replaced by the system given in Fig. 5a, so that this network can be considered as an equivalent for any meshed power system. Taking this network into account in a symmetrical or superimposed component representation, each sequence network can be considered separately like shown in Fig 5b. As presented in Fig. 2-5 the connection type of the sequence network depends on the fault type only. The meshed system can be reduced to the system from Fig. 5c. with two busbars using the commonly known wye-delta transform. During the reduction process, a fictive parallel line without mutual coupling appears between busbar A and B. In order to prove that this parallel line does not impact the calculation procedure for the compensation factors and compensation quantities, the wye-delta transform can be used. It can be noted that the calculated impedances applied to compute the compensation factors depend on the fault location. This does not limit the approach presented in this paper. However, using the estimated source impedances presumes that the fault occurs on the line between busbars A and B.

III. ACCURACY IMPROVEMENT

The compensation quantity introduced in section *A-C* corresponds to the fault current seen from side A and is deduced from the measured values on this side ($\underline{Z}_{A,0}$, $\Delta\underline{Z}_{A,1}$ or $\underline{Z}_{A,2}$). However, the compensation factor depends on the network homogeneity degree as well as on the fault location *m*. Therefore, the compensation factors require an equivalent of source impedance from side *B* in symmetrical components ($\underline{Z}_{B,0}$, $\Delta\underline{Z}_{B,1}$ or $\underline{Z}_{B,2}$), and the fault location *m*. The impedance parameters are a priori unknown because they depend on the short circuit power of the remote side and on the network configuration, which are not available to the relay. However, they can easily be obtained by implementing data exchange between both devices. This data exchange procedure offers several advantages:

- It makes network states available to each relay in order to calculate the fault current.
- It only requires the exchange of a limited number of parameters.
- It does not require synchronization of the exchanged data, as opposed to other two-side based algorithms.

Data exchange makes it possible to determine the system's state. Moreover, the parameter *m* (fault location) can be calculated using an iterative procedure. Equation (5) is divided by the reactance per unit length *x'*, which is a constant parameter of the line, in order to obtain the fault location. Introducing Gauss' method, (20) is obtained:

$$m_{n+1} = \frac{\sin\varphi \cdot \mathrm{Im}[\underline{U}_{A,Ph} \cdot \underline{I}^{*}_{A,Cmp} \cdot \underline{\delta}^{*}_{A,B}(m_n)]}{x' \cdot \mathrm{Im}[e^{j\varphi} \cdot \underline{I}_{A,Ph} \cdot \underline{I}^{*}_{A,Cmp} \cdot \underline{\delta}^{*}_{A,B}(m_n)]}, \quad m = m_{n+1} \quad if \quad |m_{n+1} - m_n| < \varepsilon \tag{16}$$

where ε is a condition for the last iteration step. With this condition, if iterations do not contribute to any improvement of the result, the fault location *m* is adopted. Considering (16), it can be noted that after some reformulations, a quadratic form for almost all fault types can be derived as well. An analytic equation of the third order only appears in the case of a phase-to-phase fault with earth. The analytical solution of such an equation is much more complex than the iterative approach. As a result, the iteration approach was chosen as general solution for the implementation of each fault type. After a successful estimation of the fault location, the fault resistance as minor product is computed.

IV. EXPERIMENTAL RESULTS

After implementing the algorithm in protection devices, tests were performed for different network structures and fault types represented by simulation models. The parameters used for the network model are typical for high voltage overhead lines. The test environment, shown in Fig. 6, is made of two test devices to which three phase currents and voltages are provided by current and voltage amplifiers [8], [9]. A communication interface without synchronization was implemented between the two devices, enabling the data exchange. The fault locator function was triggered after the pick up of the protection function [10], [11], for which distance protection was used.

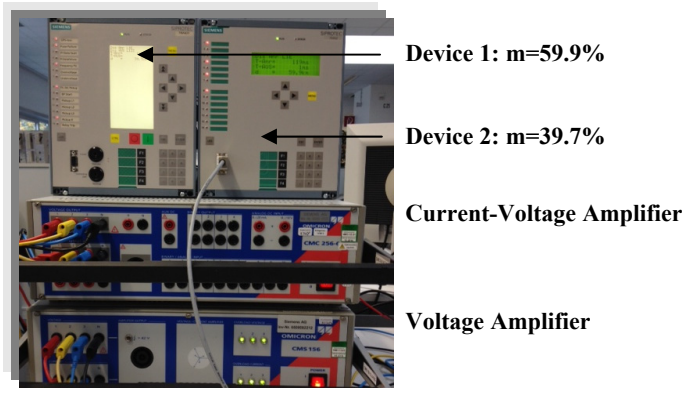

Figure 6. Test environment

The behavior of the fault locator algorithm for various fault locations has been tested for each fault type. As an example, the calculated fault location for a phase-to-earth, phase-to-phase (without and with earth) and a three-phase fault are

plotted in Fig. 7 for locations every 5% of the fault line. The fault resistance is equal to 5Ω. The representation focuses on several points, which present the greatest observed deviance. As shown in Fig. 7, the maximum error attained is of 0.8%, although the simulated system contains significant load flow (different short circuit power and phase shift between both voltage sources from Fig. 1) and inhomogeneous network.

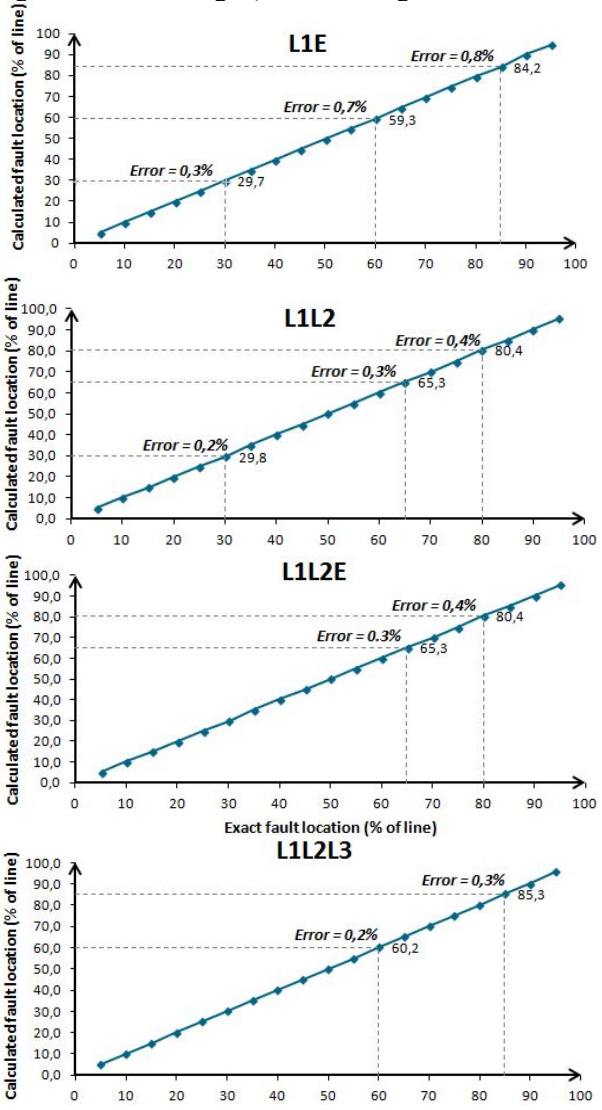

Figure 7. Calculated fault location determined with protection devices as a function of the exact fault location for each fault type L1E, L1L2, L1L2E and L1L2L3 respectively

The implemented algorithm shows very satisfying results, as it calculates precise values not only for the fault location but also for the fault resistance. The tests have been performed for various fault resistance values ranging from 1Ω to 100Ω, giving similar results as the ones presented in Fig. 7. The results showed no influence of the fault resistance on the fault location as opposed to the conventional impedance method.
Moreover, tests with meshed networks also provided accurate results for faults located on the line between the two bus bars, as the impedances calculated with the measurements from the protection relays gave an equivalent of the meshed network.

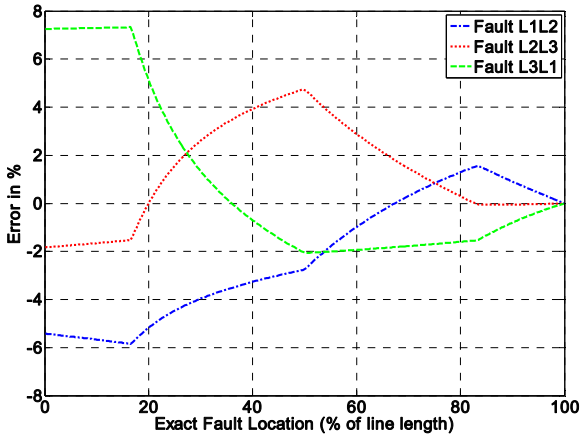

Figure 8. Calculated fault location determined with protection devices as a function of the exact fault location for each phase-to-phase fault without earth – transposed line with concentrated parameters

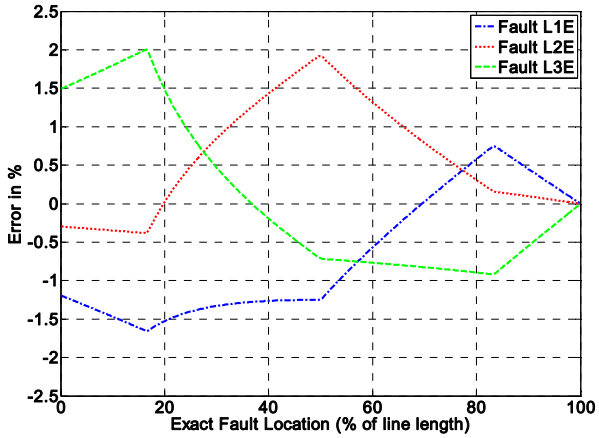

Figure 9. Calculated fault location determined with protection devices as a function of the exact fault location for each phase-to-earth fault – transposed line with concentrated parameters

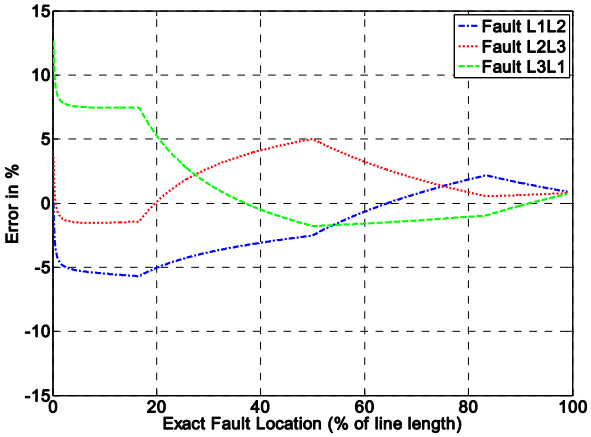

Figure 10. Calculated fault location determined with protection devices as a function of the exact fault location for each phase-to-phase fault without earth – transposed line with distributed parameters

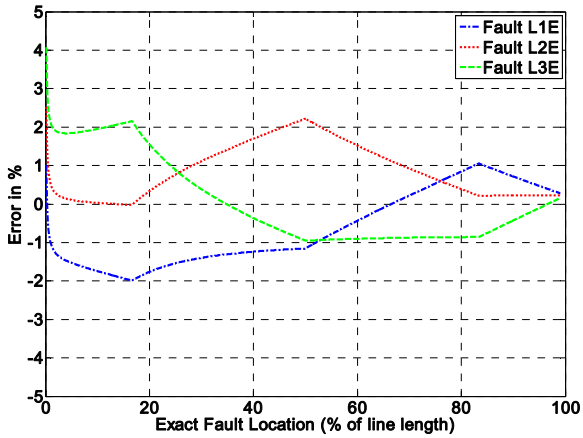

Figure 11. Calculated fault location determined with protection devices as a function of the exact fault location for each phase-to-earth fault – transposed line distirbuted parameters

For the transmission of power on long distances, transposed lines are used. Depending on the voltage level and on the line length, different transposition schemas can be applied. In order to further investigate this method, a single line from the Mexican power system (from the transmission system operator CFE) was considered. This line has three main sections that are transposed to each other. The line is fed in from both sides with a heavy load. Different fault types with fault resistances were simulated and tested, using a protection device as shown in Fig. 6. The investigation results are presented in Fig. 8-9. The line was modeled with concentrated parameters. As shown in Fig. 8-9, the iterative algorithm (16) converges to the stable fault location value. Due to transposition of the lines, an error on the fault location appears. It depends on the fault position, faulted phases and also on the fault type. This error results from line geometry. In case of a phase-to-phase fault, errors up to 8% were measured. For phase-to-earth faults, the observed errors were below 2.5%. The fault location errors (relative values) are decreasing with an increasing fault location. The reason for these errors is a parasitic effect, which results from the line's asymmetry caused by the fault. This leads to two unwanted effects: a) the fault model given in Fig. 2-4 in symmetrical components is only an approximation of the fault because of the magnetic coupling between sequence networks; b) the calculation of the source impedance with the measured values not exact. An improvement of the result in this case can only be achieved if the transposition schema and full coupling matrix is available in the protection relay. For long lines, the influence of the capacitive currents and the fact that the line parameters are distributed must also be considered. The results of these tests are presented in Fig. 10-11. It was assumed that the line is transposed. In this case, only a low deviation of the results is observed, compared to the results obtained with the model with concentrated parameters (Fig. 8-9). This confirms that the proposed method is also applicable for long lines.

V. SUMMARY

This paper focuses on the explanation of the method and its theoretical background. It has been shown that the developed algorithm efficiently calculates the faulty loop's impedance in fault location applications. Successful experimental results were obtained, also when considering typical influent factors such as load flow, fault resistance and system homogeneity degree. A significant improvement in precision of fault location is therefore achieved. The advantage of the algorithm is an elimination of the numerous aspects regarding synchronization accuracy and availability of the stable communication interface between devices. The weakness of the method is its dependency on the line parameters, which can show through the residual factor $\underline{k}_0$ or the mutual coupling of the parallel line $\underline{k}_M$. The line geometry and transposition schema can also influence the results of the fault location. Moreover, the faulty loop must be provided to fault location algorithm in order to calculate the correct fault location and fault resistance. Nevertheless, this method can be successful used in combination with other fault location algorithms and in a lot of cases guarantees a very good accuracy.

References

[1] T. Takagi, Y. Yamakoshi, M. Yamaura, R. Kondow and T. Matsushima, "Development of a New Type Fault Locator Using The One-Terminal Voltage and Current Data," *IEEE Trans. Power Apparatus and Systems*, vol. 101, pp. 2892-2897, Aug. 1982.

[2] L. Eriksson, M. M. Saha and G. D. Rockefeller, "An Accurate Fault Locator with Compensation for Apparent Reactance in the Fault Resistance Resulting from Remote-End Infeed," *IEEE Trans. Power Apparatus and Systems*, vol. 104, pp. 424-436, Feb. 1985.

[3] M. M. Saha, J. Izykowski, E. Rosolowski, *Fault Location on Power Networks*, London: Springer, 2010.

[4] J. Izykowski, *Fault Location on Power Transmission Lines*, Wroclaw Poland: Wydawnictwo Politechniki Wroclawskiej, 2008.

[5] J. Izykowski, E. Rosolowski and M. M. Saha, "Locating Faults in Parallel Transmission Lines under Availability of Complete Measurements at One End," *IEE Proc.-Gener. Transm. Distrib.* vol. 151, pp. 268-273, March. 2004.

[6] C. Dzienis, Y. Yelgin, G. Steynberg and M. Claus, "Novel Impedance Determination Method for Phase-to-Phase Loops," in *Proc. 2014 Power Systems Computation Conf.*, pp. 1-7.

[7] J. Blumschein, C. Dzienis, Y. Yelgin, "New design of distance protection for smart grid applications, " in *Proc. 2015 XII Simposio Iberoamericano Sobre Proteccion de Sistemas Electricos de Potencia*., pp 1-7.

[8] IEEE Guide for Protective Relay Application to Distribution Lines, IEEE Std. C37.230-2007, Feb. 2008.

[9] Siemens, *SIPROTEC Line Differential Protection with Distance Protection 7SD5 – Manual*, Siemens AG, Feb. 2011.

[10] G. Ziegler, *Numerical Differential Protection – Principles and Applications*, Erlangen Germany: Siemens AG, 2012.

[11] G. Ziegler, Numerical Distance Protection – Principles and Applications, Erlangen Germany: Siemens AG, 2006.